Physica C 474 (2012) 34–37

Contents lists available at SciVerse ScienceDirect

Physica C

journal homepage: www.elsevier.com/locate/physc

Anisotropic response of the moving vortex lattice in superconducting $Mo_{(1-x)}Ge_x$ amorphous films

M.I. Dolz [a,*], D.E. Shalóm [a,1], H. Pastoriza [a], D.O. López [b]

[a] Centro Atómico Bariloche, CONICET, San Carlos de Bariloche, R8402AGP Río Negro, Argentina
[b] Center for Nanoscale Materials, Argonne National Laboratory, 9700 South Cass Av., Argonne, IL 60439, USA

ARTICLE INFO

Article history:
Received 22 November 2011
Accepted 8 January 2012
Available online 16 January 2012

Keywords:
Superconductivity
2D systems
Transverse critical current
Anisotropic behavior

ABSTRACT

We have performed magnetic susceptibility measurements in $Mo_{1-x}Ge_x$ amorphous thin films biased with an electrical current using anisotropic coils. We tested the symmetry of the vortex response changing the relative orientation between the bias current and the susceptibility coils. We found a region in the DC current–temperature phase diagram where the dynamical vortex structures behave anisotropically. In this region the shielding capability of the superconducting currents measured by the susceptibility coils is less effective along the direction of vortex motion compared to the transverse direction. This anisotropic response is found in the same region where the peak effect in the critical current is developed. On rising temperature the isotropic behavior is recovered.

© 2012 Elsevier B.V. All rights reserved.

1. Introduction

The study of the dynamic behavior of elastic media in the presence of different static potentials has been center of attention in the recent years. Superconducting vortices are almost ideal systems for the study of the phenomenology of these systems because relevant properties such as density, interactions and external force can be easily controlled.

Much work has been done on the problem of moving vortex systems. Depending on the velocity and type of static potential it is expected to arise different dynamical phases. In the elastic regime, Giamarchi and Le Doussal [1] have predicted the existence of a moving-Bragg-glass phase for high driving currents and a weak disordered static potential. This is a phase free of dislocations, with a power law decay of the positional correlations which are anisotropic with respect to flow direction. On another hand, Balents et al. [2] have argued for the existence of a smectic phase. In this phase, vortices move along well defined static channels, holding correlation perpendicular to the channels, but uncorrelated along them. On increasing disorder plastic motion is expected close to the depinning force showing a mixture of moving and fixed vortices [3]. In the later case the vortex motion is also through meandered static flow patterns. A common expected feature of all these dynamical states is the anisotropic response of the moving structure to perturbations parallel or perpendicular to the vortex motion.

A number of experimental works have been done investigating these phenomena. Transport measurements report changes in the dynamical properties of the vortex matter close to the peak effect [4–7] that were attributed to a crossover from plastic to ordered motion. More recently Kokubo and coworkers [8] have proven this dynamical ordering from mode locking experiments. Snapshots of moving vortex structures have been obtained in decoration experiments [9,10] that have shown evidence for these smectic and moving glass phases of vortices. However one of the most striking properties of these quasi-ordered driven phases is the existence of barriers to a small force transverse to the direction of motion. These barriers would originate an effective transverse critical current [11] or a change in the Hall noise spectrum [12]. Although the numerical results present a clear evidence of these effects the experimental confirmation is evasive. Recently Lefebvre et al. [13] have shown transport measurements in superconducting metallic amorphous tapes that reveal the existence of a transverse critical current although these results show big quantitative discrepancies with numerical simulations.

Mutual inductance techniques have proven to be a valuable tool for measuring superconducting characteristics of two dimensional systems [14,15]. In previous works it was shown that a variation of this technique based in special shaped coils is capable of detecting the anisotropic character of dynamical phases [16,17]. In this work we extend these susceptibility measurements to $Mo_{1-x}Ge_x$ amorphous films that reveal the anisotropic characteristic of dynamical vortex phases. This technique allows the measurement

* Corresponding author. Present address: Departamento de Física, Universidad Nacional de San Luis, INFAP, CONICET, Ejército de Los Andes 950, D5700BWS San Luis, Argentina.

E-mail address: mdolz@unsl.edu.ar (M.I. Dolz).

[1] Present address: Departamento de Física, Facultad de Ciencias Exactas y Naturales, Universidad Nacional de Buenos Aires, Ciudad Autónoma de Buenos Aires, Argentina.

0921-4534/$ - see front matter © 2012 Elsevier B.V. All rights reserved.
doi:10.1016/j.physc.2012.01.005

of susceptibility and transport at the same time obtaining susceptibility information with applied current to the sample.

2. Experimental details

Mutual inductance measurements were performed using planar serpentine coils of geometry similar to those described in a previous paper [17]. It was showed that the implementation of rectangular coils with high aspect ratio allow the direct measurement of the anisotropy. Shielding currents are induced in the sample by the primary coils and therefore they are predominantly parallel to the long side of the coil, as it is shown in Fig. 1d. As a consequence the voltage generated in the reception coil is originated by the sample currents flowing in that direction. For the experiments reported in this work the coils were batch fabricated on silicon substrates and later the superconducting film was deposited on top of them. Coils with different geometries have been build using 0.5 μm thick aluminum as conducting material and SiO_2 as insulator. The fabrication process started from a 8″ silicon wafer covered with 650 nm of Low Stress silicon nitrate. Aluminum wiring of the primary coil was defined by optical lithography and lift-off. Deposition of SiO_2 by Chemical Vapor Deposition (CVD) with a nominal thickness of 2 μm was used as a first isolation layer. A second lithography step, with the same mask used previously but rotated 180° defined the secondary coil. A final SiO_2 2 μm layer was deposited to provide a second isolation layer between the coils and the superconducting film. A planarization with a Chemical Mechanical Polishing (CPM) was performed afterward. Finally vias in the SiO_2 were defined by lithography and HF etching to allow direct bonding of Au wires to each coil. In Fig. 1a we show a photograph of one of the microfabricated coils. All the results presented in this work correspond to coils with Al wires of 30 μm in width separated by 100 μm and with 30 turns.

On top of the coils the superconducting $Mo_{1-x}Ge_x$ 500 nm amorphous films were deposited by RF – sputtering at room temperature by water cooling of the sample holder. A cross shaped geometry was defined in the superconducting film by lithography and lift-off which allow the DC current injection in the film parallel and perpendicular to the coil direction. In Fig. 1b we show photograph of the sample and a scheme of the electrical contacts. Fig. 1c presents a sketch of the experimental configuration. The critical temperature of the films determined as the onset of resistance at zero magnetic field was 7.93 K.

The field and temperature dependence of the susceptibility were acquired for different applied currents to the sample for both directions: current parallel (y direction) and perpendicular (x direction) to the long strips of the coils. The voltage drop in the film was simultaneously measured using a nanovoltmeter that allows the detection of the vortex motion induced by the external current. The protocol utilized was the following: for a fixed external applied field the temperature of the sample was varied and regulated at fixed setpoints. For each of these temperature steps the current in the sample was swept in magnitude and orientation while the susceptibility and voltage drop in the sample were acquired. All measurements presented here were performed in the linear regime of the susceptibility and for a driving frequency and amplitude of 40 kHz and 0.8 mA, respectively.

3. Results and discussion

The principal result of this paper is represented in Fig. 2 where the susceptibility of the sample is plotted as a function of temperature, on measuring it with an electrical current through the sample for the two current orientations and an applied magnetic field perpendicular to the film. In the following we define $\chi_{\parallel}$ as the susceptibility data taken where the bias current is parallel to the long side of the coils (I_y, y direction), and $\chi_{\perp}$ where the bias current on the sample is perpendicular to them (I_x, x direction). The data indicate that once the vortex motion is induced by the external current the response obtained for currents parallel and perpendicular to the coils are notably different. At currents lower than 0.1 mA the magnetic response is the same to both currents orientation. Thus, this magnetic response can be taken as the reference response, $|\chi'_0|$. At currents greater than 0.1 mA the shielding capability, $|\chi'|$, is lower in the case where the external current is parallel to the long side of the coils respect to the perpendicular configuration. A lower value of the $|\chi'|$ data is an indication of an increase in the vortex mobility. Taking into account that the shielding currents induced in the sample basically mimic the geometry of the primary coil [17], the

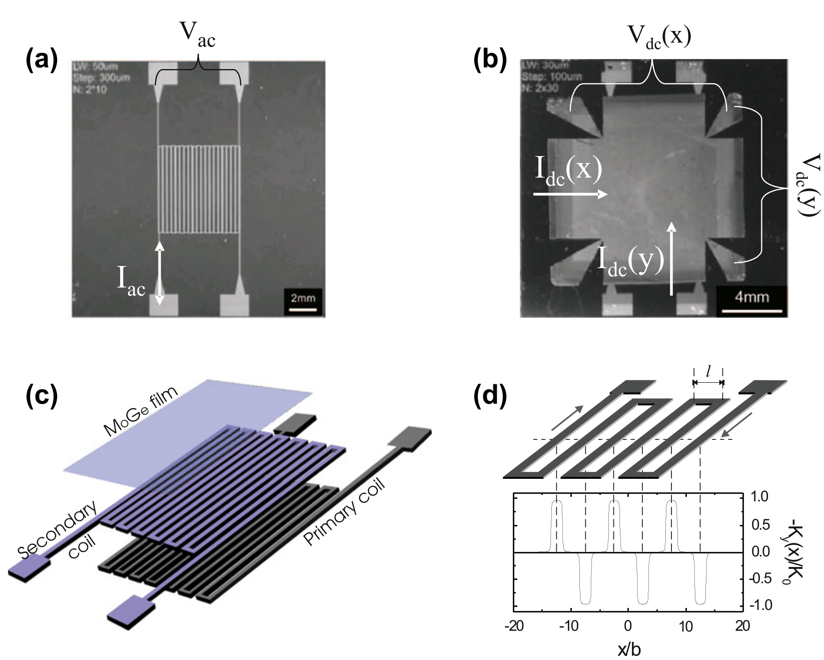

Fig. 1. (a) Photograph of the microfabricated Al coils. (b) Photograph of the superconducting amorphous film on top of the serpentine coils. Overlapped are indicated the electrical contacts. (c) Schematics of the measurement configuration. (d) Profile of the current density induced by the primary coil in the sample.

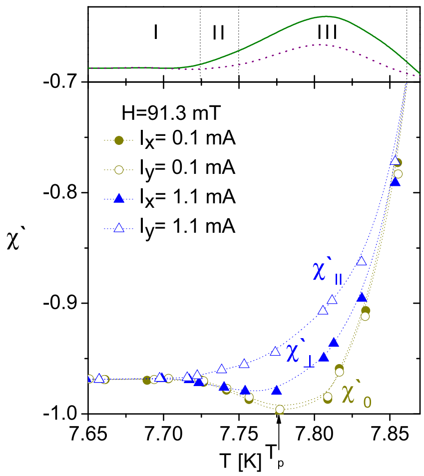

Fig. 2. Bottom panel: real part of the susceptibility taken with two bias currents in the sample of 0.1 mA and 1.1 mA for one applied magnetic field perpendicular to the film. Open symbols corresponds to the data taken when the bias current on the sample is parallel to the long side of the coils. Closed symbols: bias current perpendicular to the long side of the coils. Dotted lines are splines to the data. Top panel: Subtraction of the $\chi_{\parallel}$ and $\chi_{\perp}$ fits to the reference χ_0 fit (green and purple line respectively) showing the first three phases found. (For interpretation of the references to color in this figure legend, the reader is referred to the web version of this article.)

parallel configuration corresponds to the case that these shielding and external currents are collinear. This means that when the bias current is parallel to the long side of the coils the *dc* force and the alternate testing force generated by the currents induced in the sample by the primary coil are almost collinear. As a consequence, the results of these experiments are evidencing that the vortex mobility is greater along the vortex motion direction than perpendicular to it. An isotropic response is recovered at high temperatures where the data for both current orientations merge together and with that taken at zero current on the sample. The observed anisotropy occurs in a region where the susceptibility of reference $|\chi'_0|$ indicates an increase in the shielding capability. In Fig. 2 we can see this increment from $T = 7.73$ K, which is an evidence of the peak effect [18] where the vortex ensemble softens to accommodate to the weak pinning potential increasing the critical current.

In Fig. 3 we plot the susceptibility data for fixed temperature and magnetic field as a function of applied external current in the sample for both current orientations. The temperature, T_p was chosen as that where the susceptibility of reference (χ'_0) is

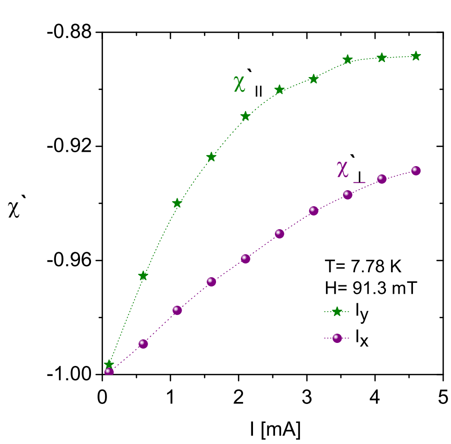

Fig. 3. Real part of the susceptibility as a function of the bias current for both current orientations at a fixed value of magnetic field. The temperature of these measurements was at the minimum of the susceptibility at zero current, T_p, indicated with an arrow in Fig. 2.

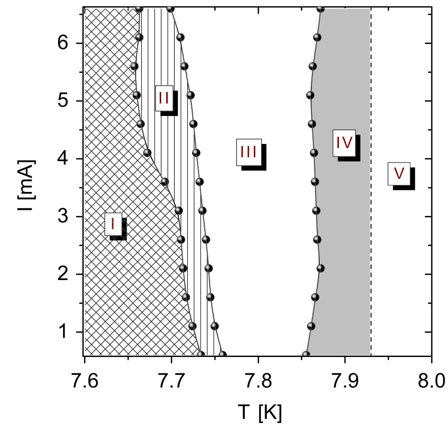

Fig. 4. Current–temperature dynamical phase diagram obtained from the electrically biased susceptibility measurements. Region I: fully pinned state, $\chi_{\parallel} = \chi_{\perp} = \chi_0$, $V_{dc} = 0$. Region II: transversally pinned state, $\chi_{\parallel} \neq \chi_{\perp} = \chi_0$. Region III: anisotropic dynamical state, $\chi_{\parallel} \neq \chi_{\perp} \neq \chi_0$. Region IV: isotropic moving phase: $\chi_{\parallel} = \chi_{\perp} = \chi_0$, $V_{dc} \neq 0$. Region V: normal state. The phase diagram is relevant only for currents above $I_{dc} = 0.5$ mA, the minimum applied current for which anisotropy is detected.

minimum (peak of the peak effect), see Fig. 2. It is clear that the anisotropic response persists in the whole range of currents investigated. At this temperature and field the longitudinal response (or parallel configuration) reaches a steady state for current values around 3.5 mA. We were not able to detect this saturation in the perpendicular configuration up to 5 mA, the maximum current up to which we were able to measure without overheating the sample. This effect (difference between parallel and perpendicular directions) could be in principle explained by an intrinsic anisotropy of the sample. However this can be discarded after observing that *I*–*V* characteristics coincide for both current directions.

More insight of the anisotropic behavior can be extracted from the analysis of the data through a subtraction of the susceptibility at a given current to a reference measurement at zero current for both current orientations, see top panel of Fig. 2. Based on this figure (and equivalent for other biasing currents), we were able to construct the *I*–*T* phase diagram shown in Fig. 4. At low temperatures the susceptibility for both current directions coincides with the measurement at zero applied current. This region I corresponds to the response of a fully pinned vortex lattice. At certain value of the external current we observe that the susceptibility measured when the current direction is along the coils long direction starts to deviate from the zero current behavior but not for the measurement in the perpendicular configuration. This result indicates that the sample is in a regime (region II) that the vortex ensemble started to move and is locked to move in the perpendicular direction proving the existence of a finite transverse critical current. Rising temperature the perpendicular susceptibility becomes different from the zero current measurement but with greater shielding capability than in the parallel measurement (region III). These results imply that this is a region of the phase diagram where the dynamical vortex structure has an anisotropic mobility. At even higher temperatures and currents an isotropic response is recovered where all susceptibilities coincide (region IV) before reaching the normal state region (V). Region IV could be assigned as a moving vortex liquid phase where pinning becomes negligible on the vortex dynamics.

4. Conclusions

Our results clearly indicate that the response of the moving vortex lattice in α-MoGe have an anisotropic characteristic in the region close to the depinning transition. Our results show the existence of two different regimes of anisotropic behavior. At lower temperatures there is a finite response in the *y* direction and the response in the perpendicular direction is current independent. This is a region where there is a transverse critical current. Rising temperature and/or the magnitude of the current, the perpendicular component *becomes depinned* but the response is still anisotropic. This anisotropic behavior coincides in the phase diagram where the peak effect in the critical current is observed.

Acknowledgments

We are very grateful to M. Hesselberth and P.H. Kes for helping us with the deposition of the MoGe films on the planar coils. This project was financially supported by CNEA and CONICET. M.I.D., D.E.S and H.P. researchers of CONICET.

References

[1] T. Giamarchi, P. Le Doussal, Phys. Rev. B 55 (1997) 6577.
[2] L. Balents, M.C. Marchetti, L. Radzihovsky, Phys. Rev. Lett. 78 (1997) 751.
[3] N. Grønbech-Jensen, A.R. Bishop, D. Domínguez, Phys. Rev. Lett. 76 (1996) 2985.
[4] S. Bhattacharya, M.J. Higgins, Phys. Rev. Lett. 70 (1993) 2617.
[5] W. Henderson, E.Y. Andrei, M.J. Higgins, S. Bhattacharya, Phys. Rev. Lett. 77 (1996) 2077.
[6] M.C. Hellerqvist, D. Ephron, W.R. White, M.R. Beasley, A. Kapitulnik, Phys. Rev. Lett. 76 (1996) 4022.
[7] M.C. Hellerqvist, A. Kapitulnik, Phys. Rev. B 56 (1997) 5521.
[8] N. Kokubo, T. Asada, K. Kadowaki, K. Takita, T.G. Sorop, P.H. Kes, Phys. Rev. B. 75 (2007) 184512.
[9] F. Pardo, F. de la Cruz, P.L. Gammel, E. Bucher, D.J. Bishop, Nature 396 (1998) 348.
[10] A.M. Troyanovski, J. Aarts, P.H. Kes, Nature 399 (1999) 665.
[11] H. Fangohr, P.A.J. de Groot, S.J. Cox, Phys. Rev. B 63 (2001) 064501.
[12] A.B. Kolton, D. Domínguez, N. Gronbech-Jensen, Phys. Rev. Lett. 83 (1999) 3061.
[13] J. Lefebvre, M. Hilke, Z. Altounian, Phys. Rev. B 78 (2008) 134506.
[14] A.F. Hebard, A.T. Fiory, Phys. Rev. Lett. 44 (1980) 291.
[15] A.T. Fiory, A.F. Hebard, P.M. Mankiewich, R.E. Howard, Appl. Phys. Lett. 52 (1988) 2165.
[16] D.E. Shalóm, H. Pastoriza, Solid State Commun. 126 (2003) 379.
[17] D.E. Shalóm, H. Pastoriza, J. Low Temp. Phys. 135 (2004) 153.
[18] J. Giapintzakis, R.L. Neiman, D.M. Ginsberg, M.A. Kirk, Phys. Rev. B 50 (1994) 16001.